$$HO_2\ (gas) \rightarrow HO_2\ (aq) \rightarrow H^+ + O_2^- \qquad (R9)$$

$$O_3\ (gas) \rightarrow O_3\ (aq) \qquad (R10)$$

$$O_2^- + O_3\ (aq) + H^+ \rightarrow OH + 2O_2 \qquad (R11)$$

[J. Lelieveld and P. J. Crutzen, *Nature* **343**, 227 (1990); P. J. Crutzen, in *Composition, Chemistry, and Climate of the Atmosphere*, H. Singh, Ed. (Van Nostrand Reinhold, New York, 1995), pp. 349–393]. Because a significant Cl source has not been identified, Cl activation on the surface of ice particles, leading to O_3 loss, appears unlikely.

17. It has been proposed that reactions involving iodine radicals derived from CH_3I play a role in tropospheric O_3 destruction [D. D. Davis *et al*., *J. Geophys. Res.* **101**, 2135 (1996)].
18. For the calculation of OH production rates we used the following parameters: water vapor mixing ratio = 18 g/kg (*15*); O_3 mixing ratios = 5 nmol/mol (Fig. 1); CO = 75 nmol/mol; and CH_4 = 1.70 μmol/mol [T. J. Bates, K. C. Kelly, J. E. Johnson, *J. Geophys. Res.* **98**, 16969 (1993)]. Measured diurnal values of the O_3 photodissociation coefficient [$J(O^1D)$] for the formation of $O(^1D)$ atoms according to reaction R1, under conditions of active convection in the Intertropical Convergence Zone of the Atlantic, were taken from A. Hofzumahaus, T. Brauers, U. Platt, and J. Callies [*J. Atmos. Chem.* **15**, 283 (1992)]. The 12-hour average was $J(O^1D) = 8.2 \times 10^{-6}$ per second. The total O_3 column densities were about 275 Dobson units for the Atlantic cruise and for CEPEX as well. Therefore, the Atlantic and the CEPEX relevant *J* values should be similar.
19. We calculated the boundary layer evacuation times for the CEPEX region using the National Center for Atmospheric Research CCM3 model (P. Rasch, personal communication) from monthly mean MBL air masses and the upward component of the deep convective mass fluxes.
20. C. A. Brock, P. Hamill, J. C. Wilson, H. H. Jonsson, K. R. Chan, *Science* **270**, 1650 (1995).
21. M. O. Andreae *et al*., *J. Geophys. Res.* **90**, 12891 (1985); S. A. Yvon, E. S. Saltzman, D. J. Cooper, T. S. Bates, A. M. Thompson, *ibid.* **101**, 6899 (1996); G. L. Gregory *et al*., *ibid*., p. 1727.
22. S. Solomon, R. R. Garcia, A. R. Ravishankara, *ibid.* **99**, 20491 (1994).
23. P. J. Crutzen and M. O. Andreae, *Science* **250**, 1669 (1990).
24. J. Fishman, K. Fakhruzzaman, B. Cros, D. Nganga, *ibid.* **252**, 1693 (1991).
25. We thank P. Rasch for supplying the estimates of the MBL evacuation times, and R. Vogt and J. Landgraf for carrying out the calculation on OH concentrations. This work was funded in part by NSF grant ATM 9405024. CEPEX was funded by NSF (ATM 8920119) and the Department of Energy (DE-F603-91ER61198).

29 May 1996; accepted 19 August 1996

Flow-Induced Molecular Orientation of a Langmuir Film

Takayuki Maruyama, Gerald Fuller,* Curtis Frank, Channing Robertson

The two-dimensional fluid dynamics of the different phases of a fatty acid monolayer (docosanoic acid) were examined. Brewster angle microscopy was used to investigate the polydomain structure of two "liquid condensed" phases (the L_2 and L_2' phases) and the "solid" (*S*) phase in situ during an extensional flow. Only the L_2 phase deformed affinely with a liquid-like response. The two other phases experienced flow-induced reorientation of the lattice onto which the molecules were arranged. The reorientation process was accompanied by the appearance of shear bands in the monolayers at an angle of ±45 degrees to the extension axis of the flow.

The flow behavior of monolayers at fluid-fluid interfaces is of fundamental and technological significance, and this subject has been reviewed at a micromechanical level by Edwards *et al.* (*1*). The influence of hydrodynamic forces on monolayers becomes apparent when their rheological responses are considered. These responses are often non-Newtonian, and shear-thinning surface viscosities are commonly encountered (*2*, *3*), providing indirect evidence of flow-induced microstructural deformation and orientation within the layer. However, in most of the earlier work in surface rheology it has been assumed that the monolayers can sustain uniform flow fields. Moreover, the approaches have been predominantly concerned with macroscopic properties, such as the surface shear viscosity and modulus. The fact that most interfaces contain mesoscopic domain structures and orientatable molecules has often been neglected.

Measurements of flow-induced orientation at the molecular level have normally been performed on Langmuir-Blodgett films where the material exposed to flow has been fixed to a solid substrate (*4*, *5*). However, such an approach does not readily lend itself to the examination of transient phenomena, and the applied flow fields are usually inhomogeneous. Here, we used in situ measurements of molecular orientation at the fluid-fluid interface and used homogeneous flow fields with well-characterized velocity gradients.

The subject of this investigation was docosanoic acid, a fatty acid that has been extensively studied with respect to its equilibrium phase behavior when residing as a monolayer at the air-water interface. Pressure-area isotherms of Langmuir films reveal a number of phase transitions, and the corresponding structures have been examined by x-ray diffraction (*6*). The latter measurements revealed the existence of mesophases having positional order but not translational order. At the temperature used in this study (15°C), two distinct, first-order transitions were evident in pressure-area isotherms: one at a surface pressure of π = 14.5 mN m^{-1} and the other at π = 27.5 mN m^{-1}. The classical assignment of the first transition is between two "liquid condensed" phases, denoted as the L_2 and L_2' phases, respectively. The second transition separates the L_2' phase from the *S* or "solid" phase. The L_2 phase has the head groups of the molecule on a distorted, hexagonal lattice with the alkyl chains' tails tilted at an angle toward their nearest lattice neighbor. As the monolayer is compressed, the tilt angle diminishes in magnitude, and across the transition the tilt direction switches toward the next nearest neighbor. As the monolayer enters the *S* phase, the tilt angle tends to zero and the alkyl chains are perfectly upright, but the head groups remain arranged on the distorted, hexagonal lattice.

The tilting of the alkyl tails of docosanoic acid makes Brewster angle microscopy (BAM) (*7*, *8*) a convenient method with which to view the polydomain structure of this system. This optical probe uses light polarized in the plane of incidence that is reflected from the interface at the Brewster angle θ_B for the substrate (water, in the case of our Langmuir films). The presence of a thin film at the interface will cause the Brewster condition to be violated and light will be reflected. If the film consists of domains characterized by unique refractive indices, the reflected light will reveal the film morphology. The reflected light is viewed through an analyzing polarizer set to an angle α relative to the plane of incidence. An angle α = 60° was found to optimize the contrast in the polydomain structure. To calculate the reflected light intensity, it is necessary to evaluate the matrix of reflection coefficients R_{ij}, $(i, j) = p$ or s, where p and s refer to light polarized parallel and perpendicular to the plane of incidence, respectively. Of interest are the off-diagonal coefficients, R_{ps} and R_{sp}, which measure the tendency to convert p-polarized light to s polarization, and vice versa. The measured intensity is

$$I = I_0[\cos^2 \alpha |R_{pp}|^2 + \sin^2 \alpha |R_{ss}|^2 + \cos \alpha \sin \alpha (R_{pp}R_{sp}^* + R_{pp}^*R_{sp})] \qquad (1)$$

where I_0 is the incident light intensity and

Department of Chemical Engineering, Stanford University, Stanford, CA 94305-5025, USA.

*To whom correspondence should be addressed.

R^*_{ij} are complex conjugates. Using the 4 × 4 matrix analysis of Berremann, we calculated the intensity reflected from an interface of tilted molecules. This is plotted in Fig. 1 as a function of φ, the angle that the tilt azimuth of the molecules makes with the plane of incidence. The parameters used in the calculation (Fig. 1) were chosen to model the properties of docosanoic acid monolayers. As seen from this plot, BAM is able to distinguish between two domains containing molecules tilted at ±90° to the plane of incidence but measures identical intensities for domains with molecules tilted parallel and antiparallel to this plane (0° and 180°). This conclusion did not change as the molecular parameters used in this calculation were varied quite extensively from their expected values. For this reason, two domains of the latter sort would appear as merged into a single area of contrast.

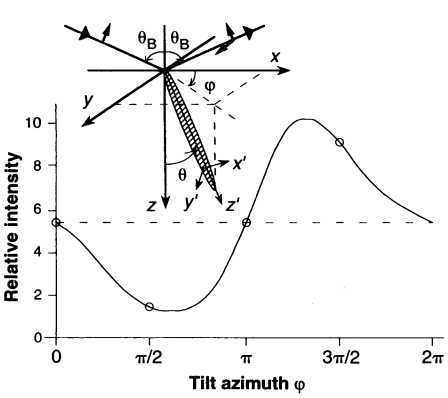

Fig. 1. The intensity of light measured by the Brewster angle microscope relative to the incident light intensity as a function of the azimuthal angle φ, defining the direction of tilt of molecules residing at the air-water interface. The angle φ is measured from the plane of incidence (the *x* coordinate in the inset). The docosanoic acid molecules were modeled as tilted at an angle θ = 20° relative to the vertical *z* direction. The refractive index of the molecules measured on the (*x*', *y*', *z*') frame shown in the inset was modeled to have principal values $n_{x'x'}$ = 2.16, $n_{y'y'}$ = 2.16, and $n_{z'z'}$ = 2.37, respectively. The monolayer was modeled to have a thickness *d* = 2.8 nm. Molecules tilted toward either φ = 0° or φ = 180° produce the same reflected light intensities, whereas the tilt directions φ = 90° and φ = 270° are distinguishable in their intensities.

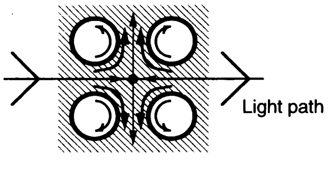

Fig. 2. Schematic diagram of the four-roll mill. The point of reflection of the light used in BAM is located at the center stagnation point of the mill, and the plane of incidence is coincident with the horizontal midplane of the mill.

We used a four-roll mill to apply extensional deformations to the monolayer. This device, developed by Taylor (9), generates a uniform, two-dimensional extensional flow. It consists of four cylinders set on the corners of a square (Fig. 2). Rotation of the rollers produces hyperbolic streamlines. The geometry and size of the device were chosen to maximize the spatial extent of homogeneous, linear flow (*10*). The four-roll mill was suspended above the Langmuir trough with the cylinders protruding through the interface. The laser beam of the Brewster angle microscope was reflected at the geometric center of the mill, where the velocity is zero but the gradient is finite. Because of the symmetry of the four-roll mill flow, any flow-induced orientations must appear at 0° or 90° relative to the flow direction.

The protocol used in the experiments was to first bring the monolayer to its desired thermodynamic state and to then subject it to a series of flow reversals during which the flow was first generated in one direction at a prescribed strain rate $\dot{\varepsilon}$ (specified by the rate of roller rotation) and strain $\dot{\varepsilon}t$, where *t* is the temporal duration of the flow. The monolayers investigated here were all sufficiently viscous so that the dynamics of the films were not affected by motion in the water subphase. In other words, the kinematics of the monolayers were driven by the rotation of the rollers and not by flow in the water below. We demonstrated this by observing the flow in the monolayer after a rapid inception or cessation of roller rotation. In such experiments, the flow of the monolayer was observed to rapidly start or stop on time scales that were respectively much faster than would be estimated for the acceleration or deceleration of the water.

Several observations were made during the deformation of the L_2 phase subject to a strain rate of 0.2 s^{-1} (Fig. 3). First, the deformation of the polydomain pattern is affine for velocity gradients above 0.2 s^{-1}, which can be established by quantitatively measuring stretching and dilation as a function of strain. For the two-dimensional, extensional flow studied here, this requires that points in the figures move according to

$$(x,y) = [x_0 \exp(\dot{\varepsilon}t), y_0 \exp(-\dot{\varepsilon}t)] \qquad (2)$$

where (x_0,y_0) are the initial coordinates of arbitrary points in the extension and compression directions, respectively. Second, the domains retain their respective light intensities, indicating that the tilt directions of the molecules do not couple to the flow. Third, the deformation is reversible, which can be established by means of a flow reversal experiment, such as shown in Fig. 4, where the interface is first strained in one direction and then strained in the reverse direction for an equal amount of strain. The system is able to return to its initial domain pattern in such an extension-compression sequence (Fig. 4). Finally, there is little measurable tendency of deformed domains to relax toward an isotropic shape after the cessation of flow, which suggests that the line tension between adjacent domains is very small. This latter point is consistent with the finding of affine deformation.

The flow behavior of the L_2' phase was qualitatively different from the dynamics of the L_2 phase. A time sequence of domain deformation during a flow reversal (Fig. 5) shows that the process is not reversible and that the final pattern (Fig. 5G) is not similar

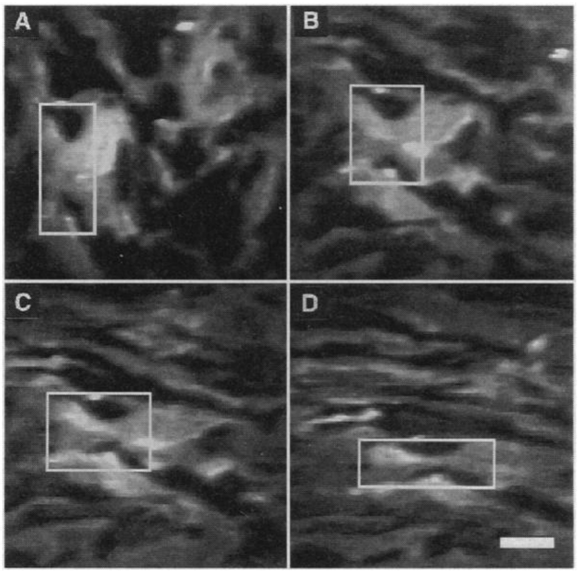

Fig. 3. BAM images of deformation of the L_2 phase domain structure subject to a strain rate of 0.2 s^{-1}. The highlighted rectangle in the figure was chosen to follow the same collection of points as they are mapped from one frame to another. The applied strain $\dot{\varepsilon}t$ in each image is as follows: (**A**) 0, (**B**) 0.6, (**C**) 0.8, and (**D**) 2.0 strain units. Analysis of the distortion of the highlighted frame confirms that the deformation of this phase is essentially affine. Scale bar, 100 μm.

to the initial pattern (Fig. 5A) even though identical strains in each direction were imposed. Close inspection of the domains during the deformation reveals the development of shear bands at ±45° to the stretching direction. These bands are characterized by a gray scale that is intermediate to the scales associated with the original domains. Moreover, the bands cut across the original domains and thicken as time progresses, until the entire image is covered at a time of 0.5 s. The result is an image such that individual domains cannot be resolved by BAM. After Fig. 5D, the flow is reversed. During the reversal, shear bands appear and a polydomain structure is recovered.

From the intensity analysis depicted in Fig. 1, it is evident that the shear bands contain molecules with tilt axes oriented perpendicular to the stretching direction. For this reason, the monolayer in Fig. 5D contains a polydomain structure that is not well resolved. The monolayers in Fig. 5, A and G, show domains in which the molecules are all either tilted upward or downward in the figure. Indeed, if the plane of incidence of the Brewster angle microscope were rotated by 90°, the microscope would resolve a polydomain pattern for the interface shown in Fig. 5D but not the structure for the interfaces in Fig. 5, A and G.

The flow fields studied here affect only the tilt azimuth and not the magnitude of the tilt angle itself. We established this by observing that the intensity contrast of domains present during flow does not change upon cessation of flow. Furthermore, domain patterns generated by flow (even those with shear bands present) do not appear to relax but remain stable in appearance once the flow is stopped. Flow is able, however, to anneal the domain structure for the case of the L_2' phase. The sequence of images shown in Fig. 5 was generated after a series of flow reversals that took an initial polydomain pattern that was similar in appearance to those shown in Figs. 2 and 3 for the L_2 phase and forced the system to a state where, although it still had a polydomain structure, the tilt azimuth angles in each domain were parallel and antiparallel to one another (as indicated by the presence of only two intensity contrasts in Fig. 5, A and G).

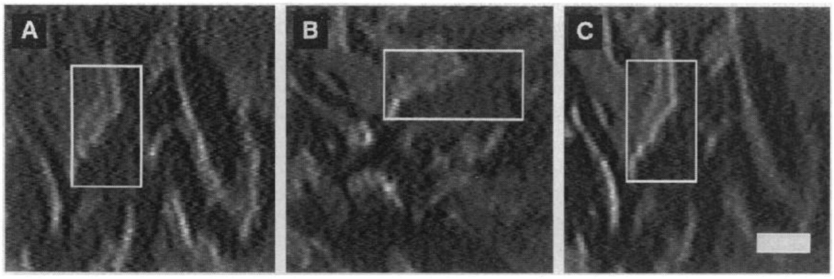

Fig. 4. BAM images of domain distortion of the L_2 phase during a flow reversal experiment. A strain rate of 1 s^{-1} was applied. In passing from (**A**) to (**B**) the system was strained horizontally by two strain units, and from (**B**) to (**C**) an opposite, vertical strain of the same amount was applied. Scale bar, 100 μm.

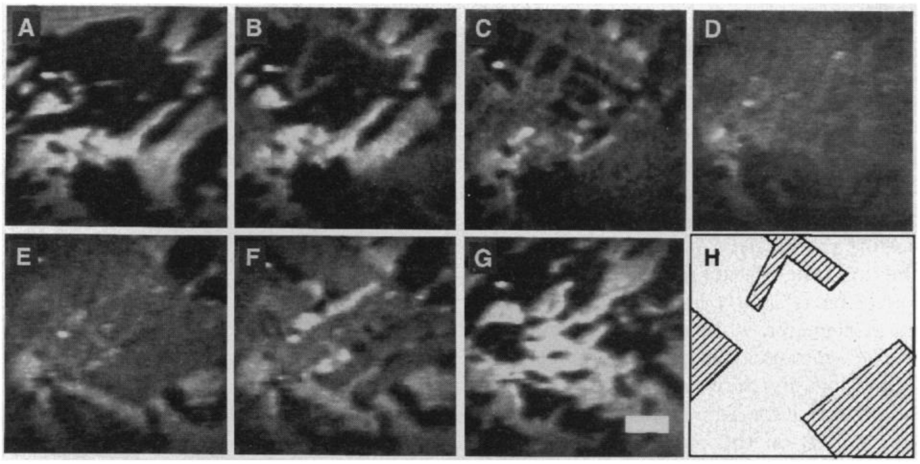

Fig. 5. BAM images of domain distortion of the L_2' phase during a flow reversal experiment. The strain rate was 1.0 s^{-1} and the applied strains were as follows: (**A**) 0, (**B**) 0.23, (**C**) 0.27, (**D**) 0.5, (**E**) 0.33, (**F**) 0.3, and (**G**) 0 strain units. For (A) through (D) the strain was perpendicular to the plane of incidence, and for (D) through (G) the strain was parallel to this plane. In this way, (G) should represent a state where the system has been returned to its initial, undeformed state. Although the contrast in the polydomain structure has been returned to its initial value, the shapes of the domains in (A) and (G) are quite different, indicating that the deformation is not affine. As the deformation progresses from (A) to (D), the contrast diminishes until it is almost completely lost in (D). The mechanism of the contrast loss is through the appearance and growth of shear bands at ±45° to the axes of strain [see (B) and (C)]. Reversal of the strain direction returns the contrast through the same mechanism. The shear bands appear as low-contrast areas in (B) and (C), whereas they appear as high-contrast areas in (E) and (F). (**H**) is a supplemental figure to clarify the shear bands in (B) as hatched areas. Scale bar in (G), 100 μm.

We also studied the response of the S phase. For this phase, the tilt angle of the molecules is zero and the BAM images show much less contrast between adjacent domains. A polydomain structure is still present, however, as a result of the placement of the molecules on a distorted, hexagonal lattice. Grain boundaries are evident in the BAM images (not shown here). Upon application of the stretching deformation, much less distortion of the structure was observed and this phase proved to be substantially more rigid than the L_2 and L_2' phases. Ultimately, once a sufficient strain was applied, shear bands were observed to appear at ±45° to the stretching direction, indicating reorientation of the lattice.

This work has considered the response to extensional deformations that lack any rotational component in the kinematics. It is anticipated that the response to a shearing deformation, composed of equal parts of extension and rotation, will lead to a dynamical response that is qualitatively different from those reported here (*11*).

REFERENCES AND NOTES

1. D. A. Edwards, H. Brenner, D. T. Wasan, *Interfacial Transport Processes and Rheology* (Butterworth-Heinemann, Stoneham, MA, 1991).
2. L. Y. Wei and J. C. Slattery, *Colloid and Interface Science* (Academic Press, New York, 1976), vol. iv, p. 399.
3. T. S. Jiang, J. D. Chen, J. C. Slattery, *J. Colloid Interface Sci.* **96**, 7 (1983).
4. V. K. Gupta, J. A. Kornfield, A. Ferencz, G. Wegner, *Science* **265**, 940 (1994).
5. S. Schwiegk, T. Vahlenkamp, Y. Xu, G. Wegner, *Macromolecules* **25**, 2513 (1992).
6. R. M. Kenn *et al.*, *J. Phys. Chem.* **95**, 2092 (1991).
7. S. Héron and J. Meunier, *Rev. Sci. Instrum.* **62**, 936 (1991).
8. D. Hönig and D. Möbius, *J. Phys. Chem.* **95**, 4590 (1991).
9. G. I. Taylor, *Proc. R. Soc. London* **146**, 501 (1934).
10. J. J. L. Higdon, *Phys. Fluids A* **5**, 274 (1993).
11. We are currently studying the responses of such a system to shearing deformations (T. Maruyama *et al.*, in preparation).

12. Supported by the NSF Materials Research Science Engineering Center on Polymer Interfaces and Macromolecular Assemblies. T.M. was sponsored by a fellowship from Bridgestone Corporation.

19 April 1996; accepted 20 August 1996